Please cite the Published Version

Gao, Z, Kulczyk-Malecka, J, Liu, H, Kelly, P, Xiao, P and Chiu, YL (2022) An amorphous SiAlN barrier coating against NaCl attack in humid air at elevated temperature. Corrosion Science, 203. p. 110321. ISSN 0010-938X

DOI: https://doi.org/10.1016/j.corsci.2022.110321

Publisher: Elsevier

Version: Accepted Version

The effect of different Ti alloys on the degradation of amorphous nitride coatings

Zhaohe Gao[a,b*],Han Liu[a], Justyna Kulczyk-Malecka[c], Conghui Liu[a], Dongchen Hu[a], Peter Kelly[c] and Ping Xiao[a*]

[a]*Henry Royce Institute, Department of Materials, University of Manchester, Manchester, M13 9PL, UK*
[b]*School of Metallurgy & Materials, University of Birmingham, Birmingham, B15 2TT, UK*
[c]*Surface Engineering Group, Manchester Metropolitan University, Manchester, M1 5GD, UK*

Abstract

Amorphous 0.9 µm thick SiAlN coatings with an Mo interlayer have been deposited on pure Ti, Ti6Al4V, and Timetal 834 alloy substrates by magnetron sputtering. After 50 h of exposure at 800°C for 10 thermal cycles in air, the SiAlN coatings on pure Ti form a thin oxide scale, whereas the SiAlN coatings on Ti6Al4V are close to being depleted, and a 0.6 µm thick remnant SiAlN coating without any signs of oxidation was observed on Timetal 834. The depletion of the SiAlN coatings induced by interfacial reaction with different substrates determines the degradation rate of the SiAlN coating, which can be retarded by Al and Sn in the Timetal 834 alloy.

Keywords: Amorphous coating; Oxidation; Degradation; Ti alloys

1. Introduction

Ti alloys are widely applied in gas turbine aeroengines and hybrid-electric airplanes due to their low density and high specific strength [1-5]. In fuel-efficient innovations for aeroengines or hybrid-electric airplanes, Ti alloys have found applications in components exposed to relatively high temperature and chemically aggressive demanding environments, e.g. as a fan blade (Ti6Al4V), compressor (Ti6242 or Timetal 834), or turbine blade (low pressure, TiAl alloys) [6-8]. However, Ti alloys have inadequate oxidation resistance at high temperatures, which restricts their applications for fuel-efficient innovations [4, 9]. Therefore, the application of Ti alloys relies on coatings technologies allowing for improved oxidation resistance of the alloys in such harsh environments [4]. Thermally stable and amorphous SiAlN (Si_3N_4/AlN, Si_3N_4 is a matrix) coatings with a Mo interlayer on Ti substrates have displayed excellent oxidation resistance in an air environment at high temperatures in our

z.gao.1@bham.ac.uk (Z.G.); p.xiao@manchester.ac.uk (P.X.)

previous work [10]. The SiAlN coating exhibited good thermal stability at high temperature as the outermost protective layer in this coating design, and the Mo interlayer provided good interfacial performance due to its diffusion into the underlying Ti substrate. However, the one-micrometer thick SiAlN layer is continuously consumed by the underlying Ti upon thermal exposure due to chemical incompatibility. Increasing the thickness of the as-deposited SiAlN layer seems to be the most obvious solution to this, but, the inherently slow deposition rate of SiAlN (e.g. ~ 1 μm per two hours) by magnetron sputtering, in comparison with the thermal spray technique, and the fact that relatively thick coatings often cause high residual stresses within the coating, restricts the maximum practical thickness of the SiAlN coating in this design [11, 12]. Therefore, the desirable approach would be to mitigate the interfacial reaction between Ti and SiAlN, and thereby the depletion of SiAlN, by introducing non-reactive alloying elements in Ti substrate.

In this study, we have deposited a series of identical 0.9 μm thick SiAlN coatings with a Mo interlayer on pure Ti, Ti6Al4V, and Timetal 834 alloys substrates by magnetron sputtering. After identical thermal exposure, the SiAlN coatings on the different substrates degrade at different speeds due to different interfacial reactions. And the effects of the alloying elements, Al and V in Ti6Al4V, Al, Sn, Zr, and Nb in Timetal 834 on the interfacial reactions have been examined.

2. Experiments and methods

The SiAlN coatings with Mo interlayers were deposited on one side of pure Ti, Ti6Al4V (wt %) alloy, and Timetal 834 (Ti-5.8Al-4Sn-3.5Zr-0.7Nb-0.5Mo-0.35Si-0.06C, wt %) alloy substrates using a UDP 350 magnetron sputtering system (Teer Coatings Ltd), equipped with 3 off 300mm x 100mm unbalanced magnetrons vertically installed through the chamber walls. Before deposition, the Ti and Ti alloy substrates were ground, polished, and ultrasonically cleaned. The polished plates were then mounted on a centrally rotating unheated substrate holder inside the sputtering chamber. The substrates were sputter cleaned at a DC bias of -600 V for 15 minutes. After cleaning, the Mo deposition was carried out in an Ar only environment with the Mo target powered by a pulsed DC power supply at a power of 500 W and 100 kHz pulse frequency, 50% duty. Following that, the deposition of SiAlN was carried out in an Ar and N_2 atmosphere, and the Si and Al targets were powered at 700 W and 300 W, respectively. During all deposition stages , a bias of -30 V was applied to the substrate holder and the substrate holder was rotated at a speed of 5 rpm, full details were reported in our previous work [10].

The SiAlN/Mo coated Ti, Ti6Al4V, and Timetal 834 coupons were tested by thermal cycling at 800°C for 5 h in air in a CM^{TM} furnace with a heating rate of 100°C / minute and followed by forced air cooling for 10 minutes (sample stage out of the heating zone), then returned for the next cycle. The cross-sectional observation of the thermal cycled SiAlN/Mo coated Ti or Ti alloys was carried out by scanning electron microscopy (SEM). To investigate the microstructure and composition of the as-deposited and thermal cycled samples, thin lamellae were prepared by FIB via a lift-out technique and then studied by transmission electron microscopy (TEM, FEI, Talos F200) fitted with a Super - X- EDS system.

3. Results and Discussion

Fig.1 a shows a cross-sectional SEM micrograph of the as-deposited SiAlN (~930 nm thick) coating with a Mo interlayer on a pure Ti substrate. The SiAlN coating shows a smooth, dense, and homogeneous microstructure without any signs of defects, as shown in Fig.1 b – b2. The Mo interlayer provides good adhesion between the nitride coating and the substrate. Identical SiAlN coatings with Mo interlayers were also deposited on Ti6Al4V and Timetal 834 alloys. The SiAlN coatings were amorphous and consisted of amorphous Si_3N_4 and AlN phases, where amorphous AlN phases are dispersed in the Si_3N_4 matrix, as reported in our previous work [10].

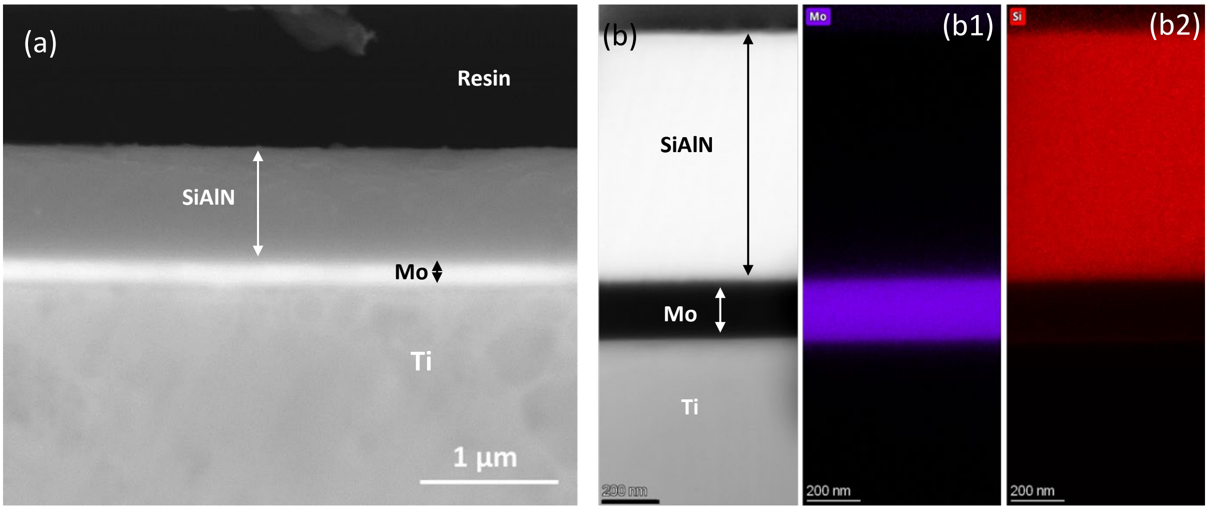

Fig. 1 Cross-sectional microstructural and compositional analysis of as-deposited SiAlN/Mo coating on Ti. (a) SEM micrograph, (b), (b1) and (b2) STEM micrograph and corresponding EDS maps.

The identical SiAlN/Mo coatings deposited on Ti, Ti6Al4V, and Timetal 834 substrates were also thermally cycled at 800°C in air to compare the effects of different substrate materials on the coatings' degradation. Figs. 2 a, b and c show cross-sectional SEM images of SiAlN/Mo coatings on Ti, Ti6Al4V, and Timetal 834 alloys, respectively, after oxidation at 800°C in air for 20 h (4 cycles). All the coated samples provide good oxidation protection in comparison with bare Ti or its alloys. However, the SiAlN coatings on different substrates degrade at different rates. SiAlN coating on Ti has been fully depleted and a thin oxide scale (~ 0.9 µm thick) has formed on top, while a ~ 250 nm thick leftover SiAlN layer was observed on Ti6Al4V and a ~ 850 nm thick remnant SiAlN layer was observed on Timetal 834, as shown in Fig. 2. Extending the thermal cycling duration from 20 h to 50 h (10 cycles), showed that the oxide scale on the SiAlN/Mo coated pure Ti thickens to ~5.0 µm, the SiAlN coating on Ti6Al4V is close to depletion, while the SiAlN coating on Timetal 834 remains considerably thicker (~0.6 µm), as shown in Fig.3 a to c and a1 to c1, respectively. It is evident that different Ti-based substrates have a significant impact on the degradation of the SiAlN coatings. Noticeably, interdiffusion and the interfacial reaction between SiAlN/Mo and the underlying Ti or Ti alloys have been observed in Fig. 2 and 3, and such interfacial diffusion/reaction is the key element to determinate the degradation rate of SiAlN coatings.

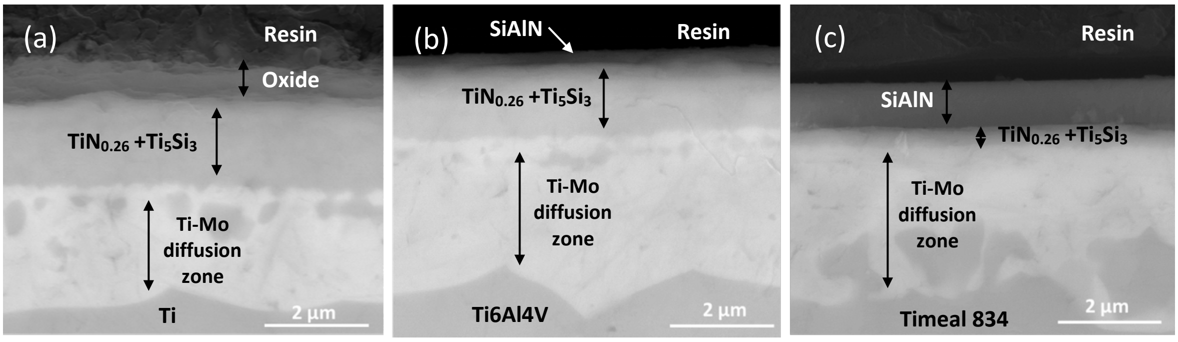

Fig. 2 Cross-sectional SEM images of SiAlN/Mo coating on different Ti alloys after oxidation at 800°C in the air for 20 h (4 cycles). (a) Pure Ti, (b) Ti6Al4V alloy, (c) Timetal 834.

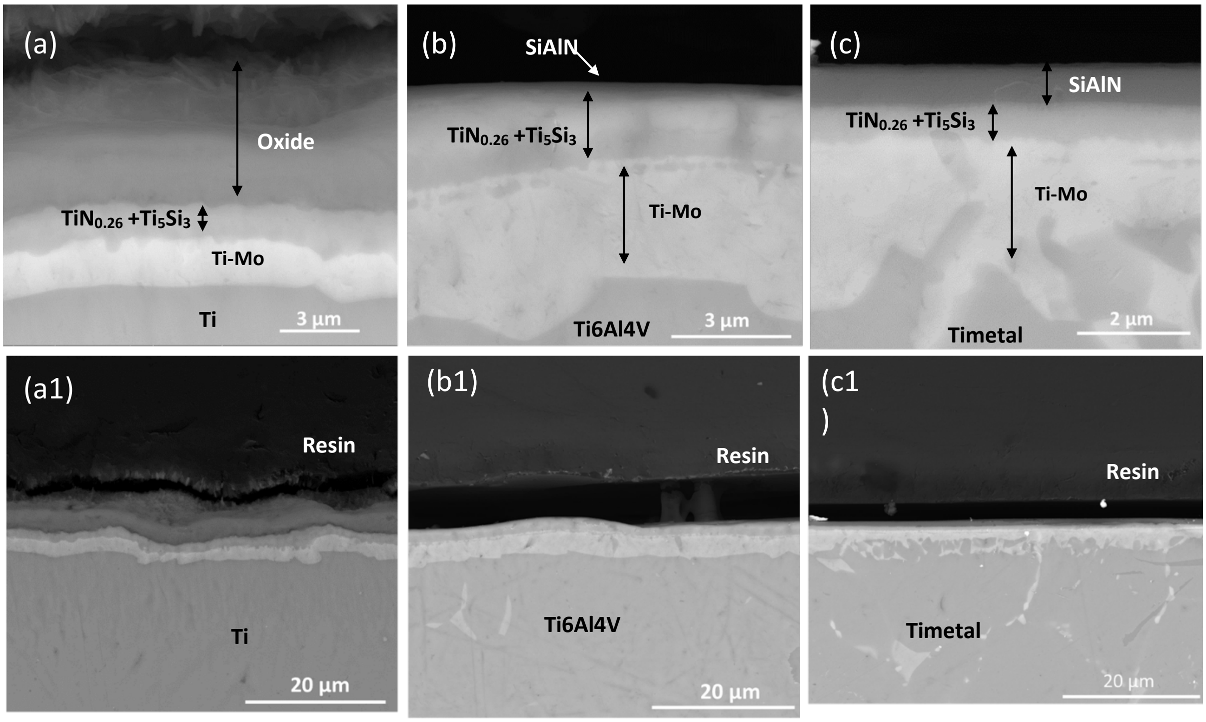

Fig.3 Cross-sectional SEM image of SiAlN/Mo coating on different Ti alloys after oxidation at 800°C in air for 50 h (10 cycles). (a) and (a1) Pure Ti, (b) and (b1) Ti6Al4V alloy, (c) and (c1) Timetal 834; a1 to c1 showing relative low magnification.

In order to examine the interfacial diffusion and reaction in finer detail, thin lamellae of cross-sections of the SiAlN/Mo coated Ti6Al4V and Timetal 834 alloys after oxidation at 800°C for 20 h (4 cycles) were prepared by FIB and studied by TEM. Fig.4 shows the cross-sectional micrographs and EDS maps of the Ti6Al4V coated alloy after oxidation at 800°C for 20 h (4 cycles). No obvious oxide scale forms on the remnant SiAlN coating and the coating has been depleted to ~ 250 nm thick, confirmed by the HAADF micrograph and EDS maps in Fig.4 a and b. During thermal exposure, the Ti-Mo interdiffusion zone can form rapidly due to the relatively high diffusivity of Mo in Ti (2.38×10^{-14} cm^2/sec, at 800°C) and the complete solubility between Mo and Ti [13, 14]. Simultaneously, Ti from the Ti-Mo zone or the Ti6Al4V (wt %) alloy can react with Si_3N_4 and AlN (matrix Si_3N_4 with minor amounts of AlN phase, below mainly consider Si_3N_4), mainly forming $TiN_{0.26}$ and Ti_5Si_3, as shown in equation 1 below, also marked in Fig.4 a and well reported in our previous work [10]. The 4 wt% (3.6 at%) V can also react with Si_3N_4, based on the Gibbs reaction energy calculated by Thermocalc, as shown in equation 2. Also, the 6 wt% (10.19 at%) Al in the Ti6Al4V alloy had been reported to react with Si_3N_4 and the reaction products are AlN and Si, as described in equation 3 [15, 16]. However, both AlN and Si can further react with Ti forming $TiN_{0.26}$ and Ti(Al) (Al is distributed in the underlying Ti as a solid solution) [10], and Ti_5Si_3, as shown in equations 4 and 5, respectively. Noticeably, there is an Al rich layer underneath the interfacial reaction zone (Fig.4 a and b, Al map) and thereby it can be expected that the Al has a retarding effect on the interfacial reaction between SiAlN and the underlying substrate.

For the Timetal 834 case, no obvious oxide scale forms on the remnant SiAlN coating after 20 h (4 cycles) oxidation, and the remaining SiAlN coating is ~ 850 nm thick, confirmed in Fig.5. The SiAlN coating on Timetal 834 depletes more slowly than that on Ti6Al4V after an identical thermal exposure. The Ti and 5.8 wt% (10.26 at%) Al in Timetal 834 can react with Si_3N_4 (SiAlN), as discussed above and described in equations 1, 3, 4 and 5. Also, the alloying elements of 3.5 wt% (1.83 at%) Zr [17] and 0.7 wt% (0.35 at%) Nb in Timetal 834 can react with Si_3N_4, as shown in equations 6 and 7, respectively. Noticeably, the 4 wt% (1.6 at%) Sn cannot react with Si_3N_4 due to the lack of proper corresponding reaction products [18, 19]. Sn has also been observed to form a Sn rich layer underneath the interfacial reaction zone, as shown in Fig. 6. Thus, it can be expected that Sn has a sluggish effect on the interfacial reaction between SiAlN and the underlying Timetal 834 substrate.

Thermodynamically, with the exception of Sn, the elements present in Ti or Ti alloys, i.e., Ti, Al, V, Zr, and Nb, can react with the Si_3N_4 from the SiAlN coating, continuously causing the interfacial depletion of the remnant SiAlN. And the outermost surface of the remnant SiAlN coating will not oxidise until it is fully consumed, due to its high activation energy and extremely low parabolic rate constant of oxidation[10] [17]. All the potential reactions between alloying elements and SiAlN have been calculated by Thermocalc (in this work only a list of some of the reaction equations is provided), and it is difficult to investigate each reaction rate considering the complexity of such a large number of reactions. Among the interfacial reactions, the reaction products between Al and Si_3N_4 can further react with the abundant Ti, described in equations 3, 4, and 5, and thereby the most thermodynamic favourable reaction are reactions 4 and 5. It can be expected that the Al from Ti6Al4V or Timetal 834 would have a relatively slower reaction rate with Si_3N_4 than that of Ti from the Ti alloys. Moreover, the activities of Ti in pure Ti, Ti6Al4V and Timetal 834 alloys were calculated, and Timetal 834 has the lowest value, followed by Ti6Al4V and pure Ti, as shown in Fig.6. Thus, the SiAlN/Mo coating on pure Ti has a relatively fast interfacial reaction rate, compared to that on Ti6Al4V, causing the complete depletion of the SiAlN coating and resulting in the formation of oxide scale. The non-reactive 4 wt% (1.6 at%) Sn along with sluggish 5.8 wt% (10.26 at%) Al in Timetal 834 alloy and the lowest Ti activity enable Timetal 834 alloy to have the slowest interfacial reaction between SiAlN and theunderlying substrates among pure Ti, Ti6Al4V, and Timetal 834 alloys.

$20.38Ti + Si_3N_4 = Ti_5Si_3 + 15.38TiN_{0.26}$ ΔG(1073.15K) = -1.09x10^{6}J/mol (1)

$5V + Si_3N_4 = V_5Si_3 + 2N_2$ ΔG(1073.15K) = -6.21x10^{4} J/mol (2)

$4Al + Si_3N_4 = 4AlN + 3\,Si$ ΔG(1073.15K) = -3.92x10^{5} J/mol (3)

$Ti + AlN \longrightarrow Ti_{1-x}Al_x + TiN_{0.26}$ ΔG(1073.15K,X=0.15, 0.15 max solid solution) = -2.93x103J/mol (4)

$5Ti + 3Si = Ti_5Si_3$ ΔG(1073.15K) = -8.16x105J/mol (5)

$6Zr + Si_3N_4 = 3Zr_2Si + 2N_2$ ΔG(1073.15K) = - 2.09x10^{5} J/mol (6)

$5Nb + Si_3N_4 = Nb_5Si_3 + 2N_2$ ΔG(1073.15K) = - 1.03x10^{5} J/mol (7)

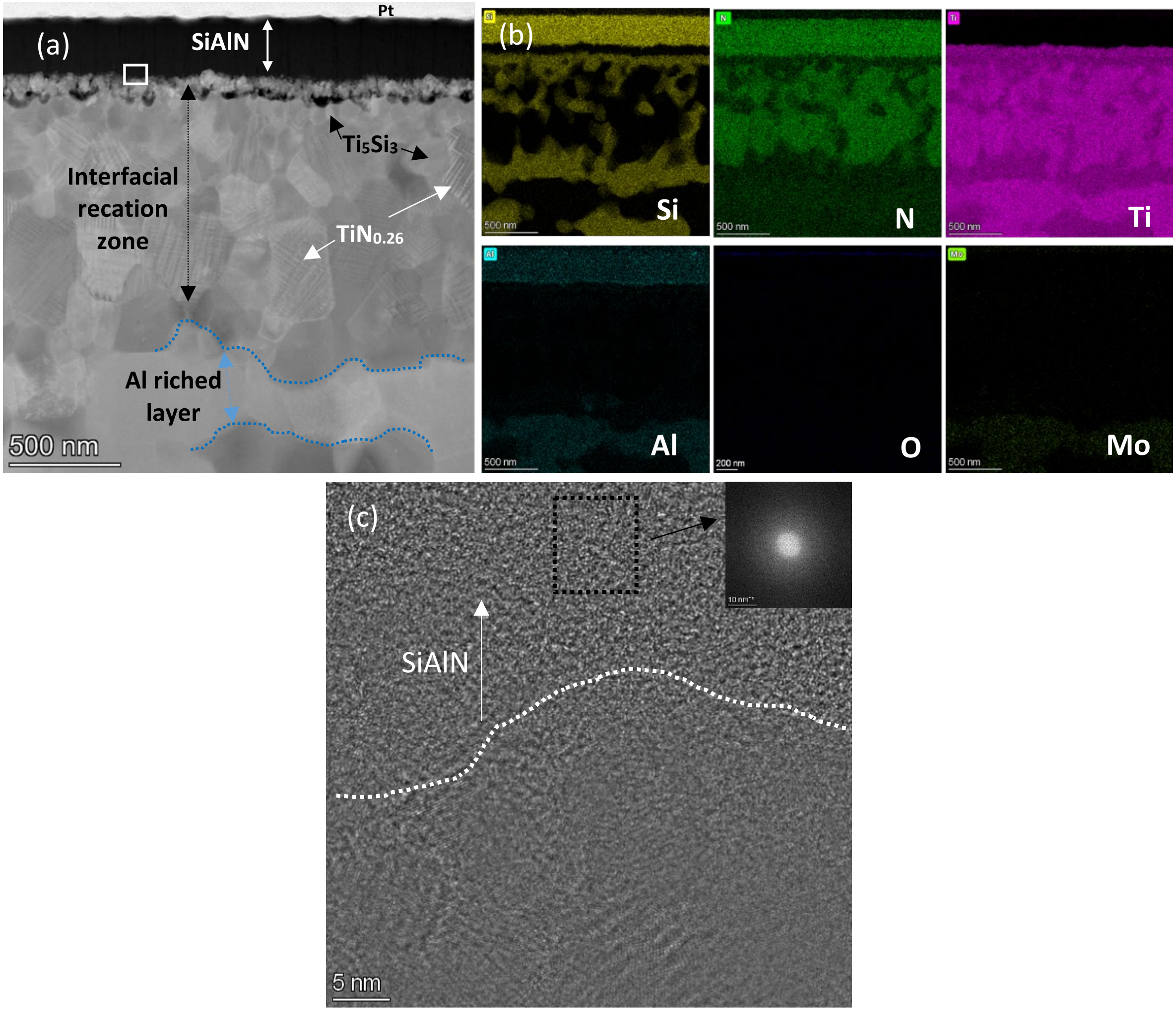

Fig.4 Cross-sectional micrographs and EDS maps of SiAlN/Mo coating on Ti6Al4V alloy after oxidation at 800°C for 20 h (4 cycles). (a) and (b) HAADF micrography and corresponding EDS maps; (c) HRTEM image, acquired from the rectangle box in (a), the corresponding FFT showing the amorphous status of the remnant SiAlN coating.

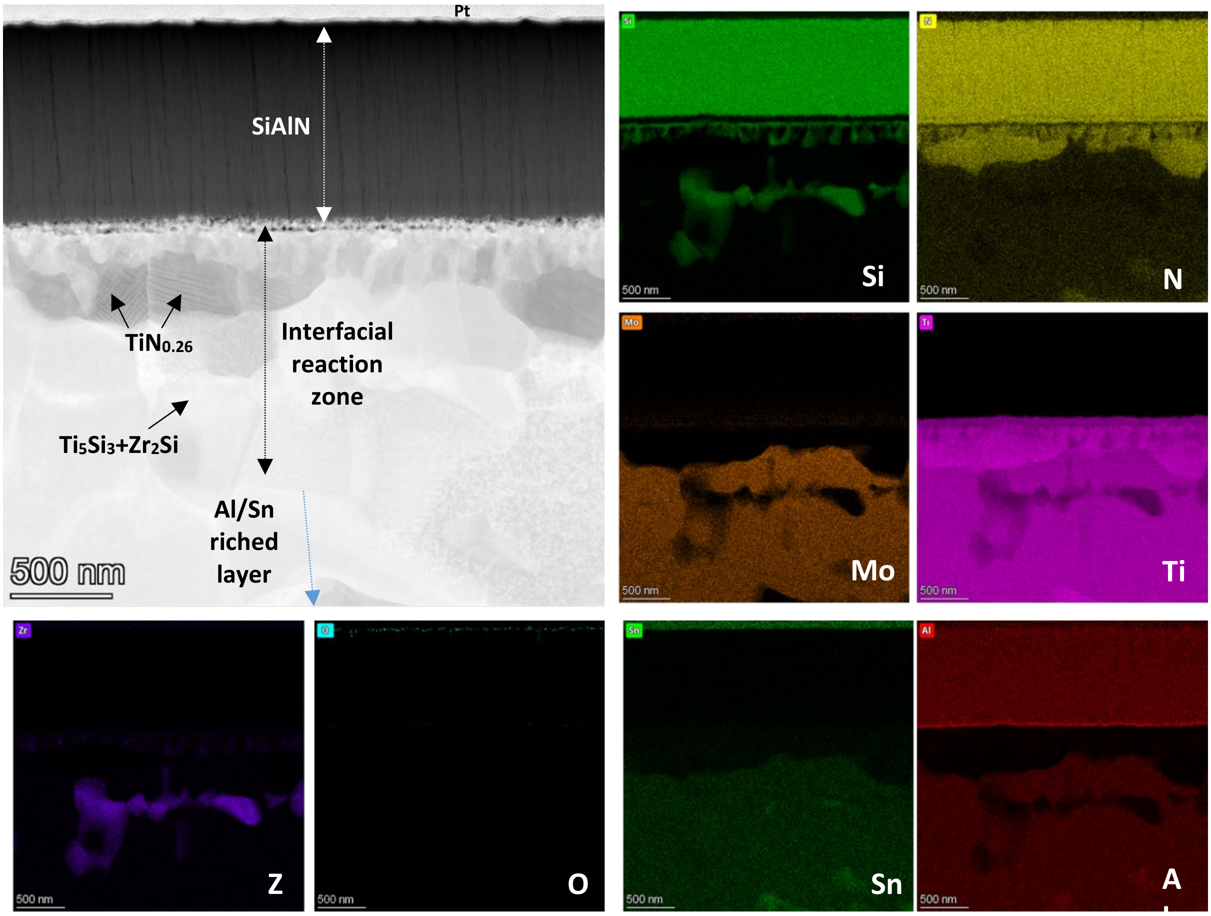

Fig. 5 Cross-sectional HAADF micrograph and EDS maps of SiAlN/Mo coating on Timetal 834 alloy after oxidation at 800°C for 20 h (4 cycles).

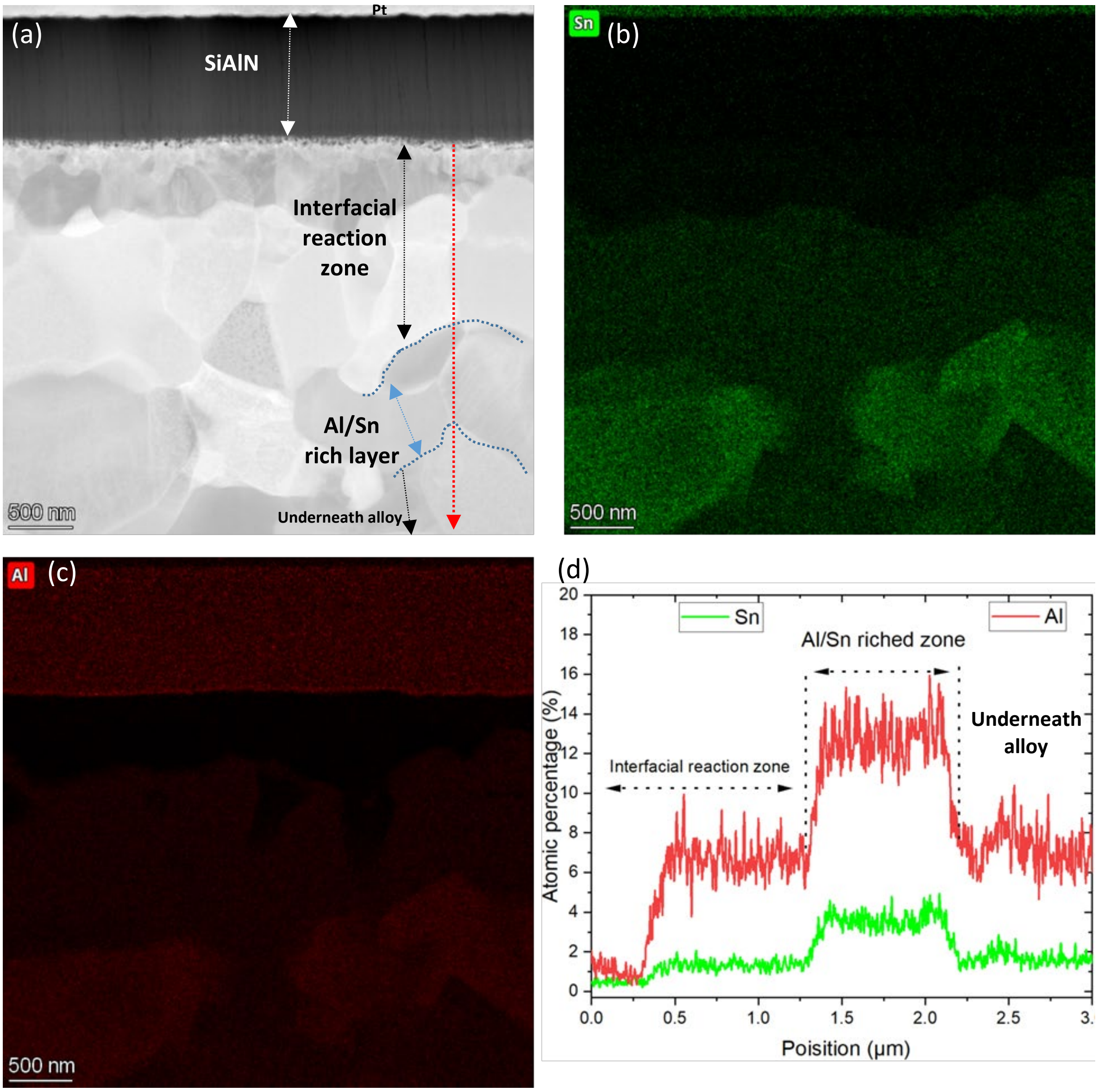

Fig.6 Cross-sectional HAADF micrograph and compositional analysis of SiAlN/Mo coating on Timetal 834 alloy after oxidation at 800°C for 20 h (4 cycles). (a), (b) and (c) HAADF micrograph and

corresponding EDS maps of Sn and Al; (d) EDS line analysis of Sn and Al, acquired from the line in (a).

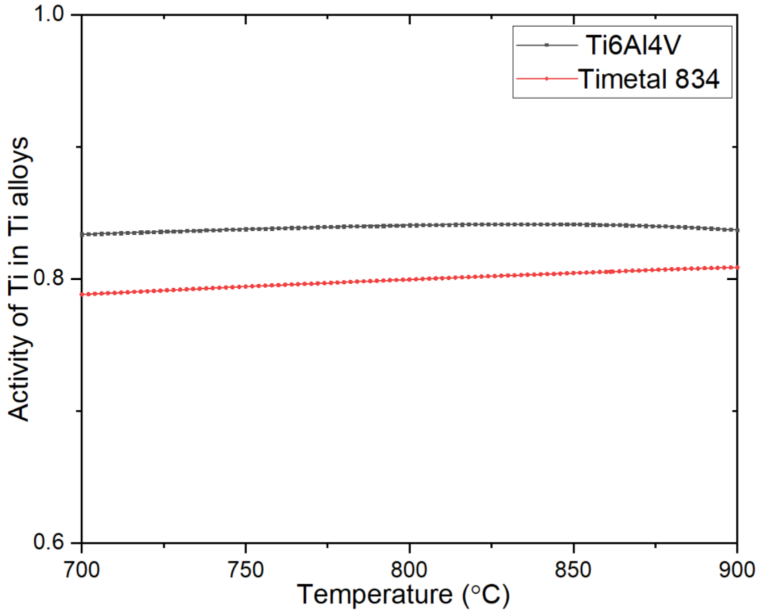

Fig.7 Activity of Ti in Ti6Al4V and Timetal 834 as function of temperature; Ti in pure Ti regarding as 1.

4. Conclusion

In conclusion, amorphous 0.9 μm thick SiAlN coatings with Mo interlayers have been deposited on pure Ti, Ti6Al4V, and Timetal 834 alloys by magnetron sputtering. The coated Ti or Ti alloys were exposed at 800°C for up to 10 thermal cycles in air. After 50 h (10 cycles), the depleted SiAlN coating on Ti forms a ~5.0 μm thick oxide scale, and the SiAlN coating on Ti6Al4V is close to being depleted, while a 0.6 μm thick remnant SiAlN coating without any oxidation has been observed on Timetal 834. The interfacial reactions between SiAlN coatings and different substrates cause the depletion of the SiAlN coating, thereby determining the degradation rate of the SiAlN coating, which can be retarded by the presence of Al and Sn in Ti alloys.

Acknowledgment

PX would like to acknowledge support from Royal Academy of Engineering and Rolls-Royce for appointment of Rolls-Royce/Royal Academy of Engineering Research Chair in Advanced Coating Technology.

Reference

[1] A. Devaraj, V.V. Joshi, A. Srivastava, S. Manandhar, V. Moxson, V.A. Duz, C. Lavender, A low-cost hierarchical nanostructured beta-titanium alloy with high strength, Nat. Commun. 7 (2016) 11176.

[2] M. Wang, Y. Lu, B. Pang, Z.T. Kloenne, H.L. Fraser, Y.L. Chiu, M.H. Loretto, Fine alpha in current and newly developed Ti alloys, Acta Materialia 173 (2019) 242-248.

[3] L. Shao, G. Xie, X. Liu, Y. Wu, Q. Tan, L. Xie, S. Xin, F. Hao, J. Yu, W. Xue, K. Feng, Combustion behavior and mechanism of Ti-25V-15Cr compared to Ti-6Al-4V alloy, Corrosion Science 194 (2022).

[4] R. Liu, Y. Cui, L. Liu, B. Zhang, F. Wang, A primary study of the effect of hydrostatic pressure on stress corrosion cracking of Ti-6Al-4V alloy in 3.5% NaCl solution, Corrosion Science 165 (2020).

[5] D. Zhang, D. Qiu, M.A. Gibson, Y. Zheng, H.L. Fraser, D.H. StJohn, M.A. Easton, Additive manufacturing of ultrafine-grained high-strength titanium alloys, Nature 576(7785) (2019) 91-95.

[6] J.A. Hooker, P.J. Doorbar, Metal matrix composites for aeroengines, Mater. Sci. Technol. 16(7-8) (2013) 725-731.

[7] G. Chen, Y. Peng, G. Zheng, Z. Qi, M. Wang, H. Yu, C. Dong, C.T. Liu, Polysynthetic twinned TiAl single crystals for high-temperature applications, Nat. Mater. 15(8) (2016) 876-81.

[8] J.C. Williams, E.A. Starke, Progress in structural materials for aerospace systems, Acta Materialia 51(19) (2003) 5775-5799.

[9] W. Li, S. Zhu, C. Wang, M. Chen, M. Shen, F. Wang, SiO2–Al2O3–glass composite coating on Ti–6Al–4V alloy: Oxidation and interfacial reaction behavior, Corrosion Science 74 (2013) 367-378.

[10] Z. Gao, Z. Zhang, X. Zhang, J. Kulczyk-Malecka, H. Liu, P. Kelly, P.J. Withers, P. Xiao, A conformable high temperature nitride coating for Ti alloys, Acta Mater. 189 (2020) 274-283.

[11] J. Musil, Hard nanocomposite coatings: Thermal stability, oxidation resistance and toughness, Surf. Coat. Technol. 207 (2012) 50-65.

[12] P.H. Mayrhofer, C. Mitterer, L. Hultman, H. Clemens, Microstructural design of hard coatings, Progress in Materials Science 51(8) (2006) 1032-1114.

[13] W.W. Xu, S.L. Shang, B.C. Zhou, Y. Wang, L.J. Chen, C.P. Wang, X.J. Liu, Z.K. Liu, A first-principles study of the diffusion coefficients of alloying elements in dilute alpha-Ti alloys, Phys. Chem. Chem. Phys. 18(25) (2016) 16870-81.

[14] J.-W. Lu, Y.-Q. Zhao, P. Ge, H.-Z. Niu, Microstructure and beta grain growth behavior of Ti–Mo alloys solution treated, Mater. Charact. 84 (2013) 105-111.

[15] Y. Lu, J. Yang, W. Lu, R. Liu, G. Qiao, C. Bao, The mechanical properties of co-continuous Si3N4/Al composites manufactured by squeeze casting, Materials Science and Engineering: A 527(23) (2010) 6289-6299.

[16] J. Avila, J.L. Sacedón, Reactivity at the Al/Si3N4 interfaces, Applied Physics Letters 66(6) (1995) 757-759.

[17] Z. Gao, J. Kulczyk-Malecka, Z. Zhang, H. Liu, X. Zhang, Y. Chen, P. Hill, P. Kelly, P. Xiao, Oxidation and degradation of amorphous SiAlN coating via forming Si-Si bond, Corros. Sci. 183 (2021).

[18] J. Liu, C. Dong, X. Lu, Z. Qiao, F. Zhou, W. Liu, R. Riedel, Sn-containing Si3N4-based composites for adaptive excellent friction and wear in a wide temperature range, Journal of the European Ceramic Society 42(3) (2022) 913-920.

[19] M.H.G. Jacobs;, P.J. Spencer, A thermodynamic evaluation of the system Si-Sn, Calphad 20 (1996) 89-91.